

# Constraining Variations in the Fine-Structure Constant with the Cosmic Microwave Background

Manoj Kaplinghat,<sup>1</sup> Robert J. Scherrer,<sup>1,2,3</sup> and Michael S. Turner<sup>3,4</sup>

<sup>1</sup>*Department of Physics, The Ohio State University, Columbus, OH 43210*

<sup>2</sup>*Department of Astronomy, The Ohio State University, Columbus, OH 43210*

<sup>3</sup>*NASA/Fermilab Astrophysics Center, Fermi National Accelerator Laboratory, Batavia, IL 60510*

<sup>4</sup>*Departments of Astronomy and Astrophysics and of Physics, Enrico Fermi Institute, University of Chicago, Chicago, IL 60637-1433*

(August 18, 2018)

Any time variation in the fine-structure constant alters the ionization history of the universe and therefore changes the pattern of cosmic microwave background fluctuations. We calculate the changes in the spectrum of these fluctuations as a function of the change in  $\alpha$ , and we find that these changes are dominated by the change in the redshift of recombination due to the shift in the binding energy of hydrogen. We estimate the accuracy with which the next generation of cosmic microwave background experiments might constrain any variation in  $\alpha$  at  $z \sim 1000$ . We find that such experiments could potentially be sensitive to  $|\Delta\alpha/\alpha| \sim 10^{-2} - 10^{-3}$ .

## I. INTRODUCTION

Physicists have long speculated that the fundamental constants of nature are not constant, but might vary with time [1]. Among the possibilities that have received the greatest attention is the time-variation of the fine-structure constant  $\alpha \equiv e^2/\hbar c$ . The best laboratory limits on  $\Delta\alpha/\alpha$  give  $|\Delta\alpha/\alpha| < 1.4 \times 10^{-14}$  over a period of 140 days [2]. Limits over a longer timescale can be obtained from astrophysical observations. In particular, spectra from high-redshift quasar absorption lines give limits of  $|\Delta\alpha/\alpha| < 3 \times 10^{-6}$  at redshifts of  $z = 0.25$  and  $z = 0.68$  [3], and  $|\Delta\alpha/\alpha| < 3.5 \times 10^{-4}$  for  $z \sim 3$  [4], with a claimed detection at the level of  $\Delta\alpha/\alpha = -1.5 \pm 0.3 \times 10^{-5}$  for a set of redshifts  $0.5 < z < 1.6$  [5].

More stringent but also more indirect limits may be placed from geology and cosmology. The Oklo natural nuclear reactor yields a constraint of  $-0.9 \times 10^{-7} < \Delta\alpha/\alpha < 1.2 \times 10^{-7}$ , between a time of 1.8 billion years ago and the present [6]. Primordial nucleosynthesis gives  $|\Delta\alpha/\alpha| < 1.0 \times 10^{-4}$  at a redshift on the order of  $10^9 - 10^{10}$  [7].

In this paper, we consider the constraints on  $\Delta\alpha/\alpha$  that could be derived from future observations of cosmic microwave background (CMB) anisotropies. Given the plethora of other constraints, is there any reason to examine CMB limits on  $\Delta\alpha/\alpha$ ? If  $\dot{\alpha}$  is assumed to be constant, then the limits quoted above correspond to  $|\dot{\alpha}/\alpha| < 3.7 \times 10^{-14}/\text{yr}$  (laboratory) [2],  $|\dot{\alpha}/\alpha| < 5 \times 10^{-16}/\text{yr}$  (quasar absorption) [3],  $|\dot{\alpha}/\alpha| < 5 - 7 \times 10^{-17}/\text{yr}$  (Oklo) [6], and  $|\dot{\alpha}/\alpha| < 1 \times 10^{-14}/\text{yr}$  (primordial nucleosynthesis) [7]. (Here we adopt  $H_0 = 75 \text{ km/sec/Mpc}$ , for consistency with ref. [3]) Our potential CMB limits will not be competitive with any of these. However, in the absence of a particular model for changes in  $\alpha$ , there is no reason to take  $\dot{\alpha}$  to be constant. Models have been proposed, for example, in which  $\alpha$  oscillates [8]. If the value of  $\alpha$  is coupled to a scalar field which evolves on cosmological timescales, then it is conceivable that  $\alpha$  could vary as a power law in the cosmological scale factor [9]. One could also imagine models in which the scalar field evolves rapidly at early times but later settles into a minimum, producing a fine-structure constant which varies at high redshifts, but settles down to a nearly constant value at low redshifts.

It is useful, therefore, to obtain limits on  $\Delta\alpha/\alpha$  at redshifts  $z \gg 1$ . The only limit of this type is provided by primordial nucleosynthesis [7]; however, that limit is very model-dependent, relying on a particular model for the dependence of the neutron-proton mass difference on  $\alpha$ . Here we present a much more direct limit, based on changes in the spectrum of CMB anisotropies which could be observed by future experiments.

In the next section, we explain how changes in  $\alpha$  alter the recombination scenario, and thus, the CMB spectrum. To simplify our discussion, we assume that  $\alpha$  has a constant (different) value throughout the recombination epoch; i.e., we neglect the possibility that  $\alpha$  changes substantially during recombination. In Sec. 3, we calculate the  $C_l$  spectrum for different values of  $\alpha$  and explain why our results look the way they do. In Sec. 4, we estimate the limits which might be placed on  $\Delta\alpha/\alpha$  at  $z \sim 1000$ . We find that the MAP and PLANCK experiments might be able to reach sensitivities of  $|\Delta\alpha/\alpha| \sim 10^{-2} - 10^{-3}$ .

## II. CHANGES IN THE RECOMBINATION SCENARIO

The fine-structure constant  $\alpha$  alters the CMB fluctuations only to the extent that it enters into the expression for the differential optical depth  $\dot{\tau}$  of photons due to Thomson scattering:

$$\dot{\tau} = x_e n_p c \sigma_T, \quad (1)$$

where  $\sigma_T$  is the Thomson scattering cross-section,  $n_p$  is the number density of electrons (both free and bound) and  $x_e$  is the ionization fraction. Thus,  $x_e n_p$  is the number density of free electrons. The Thomson cross section depends on  $\alpha$  through the relation

$$\sigma_T = 8\pi\alpha^2 \hbar^2 / 3m_e^2 c^2. \quad (2)$$

The dependence of  $x_e$  on  $\alpha$  is more complicated. Naively, one might expect  $x_e$  to scale simply with the binding energy of hydrogen, which goes as  $B = \alpha^2 m_e c^2 / 2$ , suggesting  $x_e(T, \alpha) = x_e(T/\alpha^2)$ . We will see that this is roughly correct, but it is not exact, because the recombination rates depend on  $\alpha$ . The reason that  $x_e$  depends on these rates is because it does not track its equilibrium value exactly during recombination.

Consider the standard ionization equation for Hydrogen [10]- [11]:

$$-\frac{dx_e}{dt} = \mathcal{C} \left[ \mathcal{R} n_p x_e^2 - \beta (1 - x_e) \exp\left(-\frac{B_1 - B_2}{kT}\right) \right], \quad (3)$$

where  $\mathcal{R}$  is the recombination coefficient,  $\beta$  is the ionization coefficient,  $B_n$  is the binding energy of the  $n^{\text{th}}$  H-atom level and  $n_p$  is the sum of free protons and H-atoms. The Peebles correction factor ( $\mathcal{C}$ ) accounts for the effect of the presence of non-thermal Lyman- $\alpha$  resonance photons; it is defined as

$$\mathcal{C}(\alpha) = \frac{1 + A}{1 + A + C} = \frac{1 + K\Lambda(1 - x_e)}{1 + K(\Lambda + \beta)(1 - x_e)}. \quad (4)$$

In the above,  $K = H^{-1} n_p c^3 / 8\pi\nu_{12}^3$  (where  $\nu_{12}$  is the Lyman- $\alpha$  transition frequency) is related to the expansion time scale of the universe, while  $\Lambda$  is the rate of decay of the 2s excited state to the ground state via 2 photons [12]. Clearly,  $K$  scales as  $\alpha^{-6}$  because  $\nu_{12}$  scales as  $\alpha^2$ . Furthermore it can be ascertained that  $\Lambda$  scales as  $\alpha^8$  [14]. To investigate  $\beta$ , one must first use the principle of detailed balance to relate the ionization and recombination coefficients as

$$\beta = \mathcal{R} \left( \frac{2\pi m_e kT}{h^2} \right)^{3/2} \exp\left(-\frac{B_2}{kT}\right), \quad (5)$$

while the recombination coefficient can be expressed as

$$\mathcal{R} = \sum_{n,\ell}^* \frac{(2\ell + 1)8\pi}{c^2} \left( \frac{kT}{2\pi m_e} \right)^{3/2} \exp\left(\frac{B_n}{kT}\right) \int_{B_n/kT}^{\infty} \frac{\sigma_{n\ell} y^2 dy}{\exp(y) - 1}, \quad (6)$$

where  $\sigma_{n\ell}$  is the ionization cross-section for the  $(n, \ell)$  excited level [13]. In the above, the asterisk on the summation indicates that the sum from  $n = 2$  to  $\infty$  needs to be regulated. Physically this comes about due to plasma effects which change the ionization and recombination cross-sections (calculated by considering isolated atoms). In essence, the summation gets truncated after a certain number of levels. For the present purposes, it suffices to realize that the effect of this truncation scheme depends weakly on  $\alpha$  and can be neglected [15].

The  $\alpha$  dependence of the cross-section ( $\sigma_{n\ell}$ ) can be summarized as  $\sigma_{n\ell} \sim \alpha^{-1} f(h\nu/B_1)$ , which leads to the equation:

$$\frac{\partial \mathcal{R}(T)}{\partial \alpha} = \frac{2}{\alpha} \left( \mathcal{R}(T) - T \frac{\partial \mathcal{R}(T)}{\partial T} \right). \quad (7)$$

This relation is very useful because it allows one to use the temperature parametrizations of  $\mathcal{R}(T)$  in the literature. In particular,  $\mathcal{R}(T)$  can be well fit by a power law of the form  $T^{-\xi}$ . Then from equation (7), we see that the  $\alpha$  dependence of  $\mathcal{R}$  is just  $\mathcal{R} \propto \alpha^{2(1+\xi)}$ . Let the change in  $\alpha$  be characterized by  $\Delta_\alpha \equiv \Delta\alpha/\alpha \ll 1$ ; then the corresponding fractional change in  $\mathcal{R}$  is  $2\Delta_\alpha(1 + \xi)$ . As it turns out, the results are not sensitive to the precise value of  $\xi$ , which we take to be 0.7. Thus, to first order in the change in  $\alpha$ , it suffices to consider that  $\mathcal{R}(T) \sim T^{-0.7}$ . The ionization equation (3) with the change in  $\alpha$  can be expressed as

$$-\frac{dx_e}{dt} = \mathcal{C}' \left[ \mathcal{R}n_p x_e^2 - \beta_{\text{eff}}(1 - x_e) \exp\left(-\frac{B_1 - B_2}{kT}\right) \right], \quad (8)$$

where  $\mathcal{C}' = (2\Delta_\alpha(1 + \xi) + 1)\mathcal{C}(\alpha + \Delta\alpha)$  and  $\beta_{\text{eff}}$  is the effective ionization coefficient defined as

$$\beta_{\text{eff}} = \beta \exp\left(-\frac{B_1}{kT}(2\Delta_\alpha + \Delta_\alpha^2)\right). \quad (9)$$

We have integrated equation (8) using CMBFAST [16] to derive  $x_e$  as a function of redshift for several different values of  $\alpha$ . The results are displayed in Fig. 1.

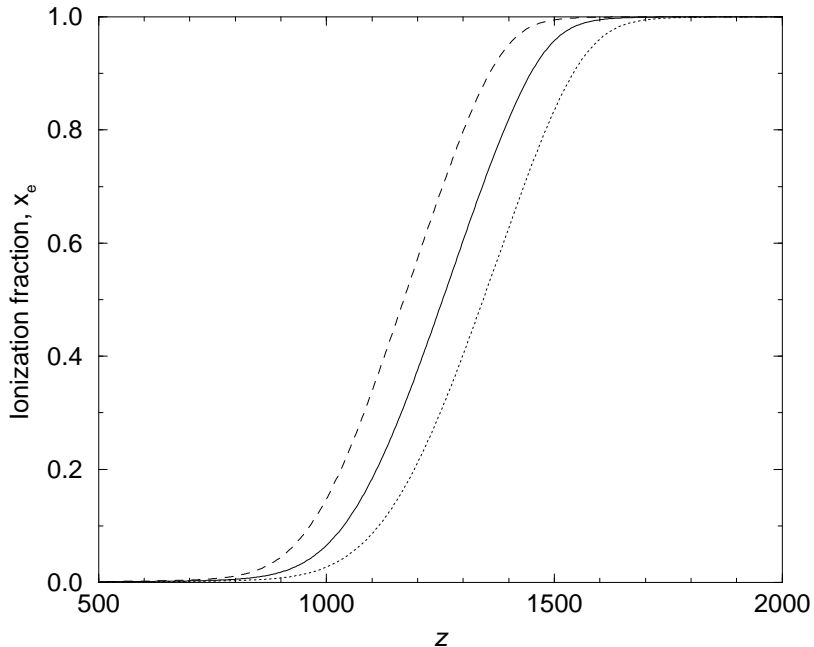


FIG. 1. The ionization fraction  $x_e$  as a function of redshift  $z$  for the standard scenario (SCDM,  $\Omega_b = 0.05$ ,  $h = 0.65$ ) (solid curve), an increase of  $\alpha$  by 3% (dotted curve), and a decrease of  $\alpha$  by 3% (dashed curve).

The most important feature, the shifting of  $x_e(z)$  to higher  $z$  when  $\alpha$  is increased, is easy to understand. Because the equilibrium ionization fraction,  $x_e^{EQ}$ , is a reasonable approximation to  $x_e$ , and  $x_e^{EQ} \propto (m_e/T)^{3/2} \exp(-B/T)$ , which is dominated by the exponential factor near recombination, to a good approximation  $x_e(z)$  is simply a function of  $z/\alpha^2$  (see Fig. 2).

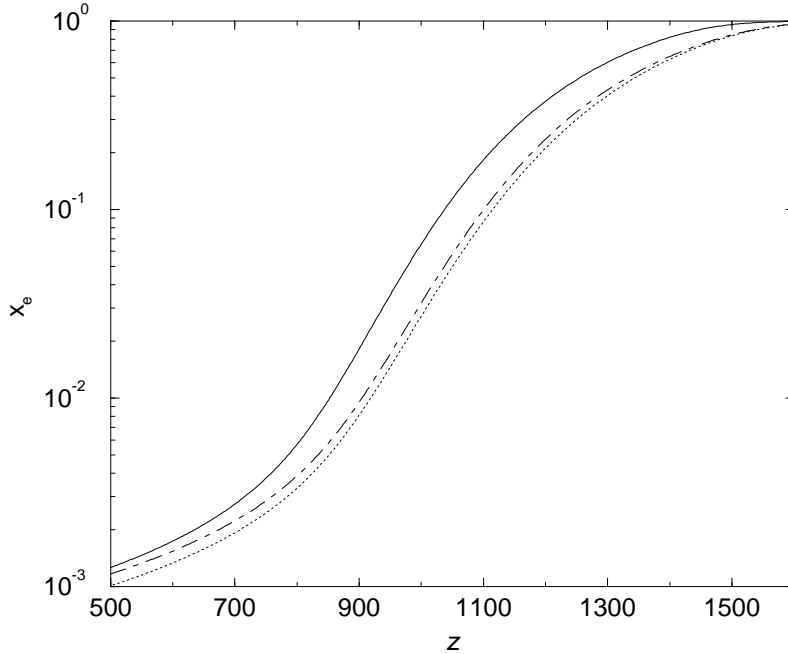


FIG. 2. A comparison of the effect on  $x_e$  of changing  $\alpha$  by +3% (dotted curve) with a simple rescaling of the redshift by  $\alpha^2$  (dot-dashed curve). Solid curve is the original ionization fraction.

As can be seen in Fig. 2, this scaling is not exact. Two effects spoil it: 1) the factor of  $(m_e/T)^{3/2}$  in  $x_e^{EQ}$ , and 2) the fact that  $x_e$  does not precisely track  $x_e^{EQ}$ . Changing  $\alpha$  not only changes the energy levels of hydrogen, but also all matrix elements and thereby the Thomson cross section and recombination rates. An increase in  $\alpha$  increases the recombination rates and so equilibrium is more closely tracked. (This can be seen from the fact that the residual ionization fraction is smaller for larger  $\alpha$ ).

More relevant for the CMB anisotropy is the visibility function,  $g(z) = e^{-\tau(z)} d\tau/dz$ , which measures the differential probability that a photon last scattered at redshift  $z$ . The visibility function depends upon  $x_e$  and  $\sigma_T$  through  $\tau$  (equation 1). The peak of  $g(z)$  defines the location of the surface of last scattering and its width determines the thickness of the last scattering surface. The finite thickness of the last scattering surface leads to the damping of the CMB anisotropy on small scales by smearing out temperature differences on these scales.

The shape of  $g(z)$  is determined largely by  $x_e$ : around the time of last scattering, the photon mean free path is very short until  $x_e \rightarrow 0$ , and the paucity of free electrons makes Thomson scattering rare. Increasing  $\alpha$  affects  $g(z)$  in three ways: first and most importantly, it shifts  $g(z)$  to higher redshift because  $x_e^{EQ}$  is shifted to higher redshift (by the approximate scaling  $z/\alpha^2$ ); second, the larger Thomson cross section increases the opacity by an overall factor, which slightly pushes  $g(z)$  to lower redshift; and finally, the shape of the  $g(z)$  curve is changed because  $x_e$  more closely tracks  $x_e^{EQ}$  for larger  $\alpha$ .

Fig. 3 shows the visibility function expressed as a function of conformal time,  $\eta$ , for different values of  $\alpha$ . This is a convenient way to display it, because the width corresponds to the comoving damping scale. Increasing  $\alpha$  shifts  $g(z)$  to higher redshift (as explained above); at higher redshift the expansion rate is faster,  $H(z) \propto (1+z)^{3/2}$ , and so the temperature and  $x_e$  decrease more rapidly, making  $g(z)$  narrower. The width of the visibility function is predicted to scale approximately as  $1/\alpha$ , which is consistent with our results.

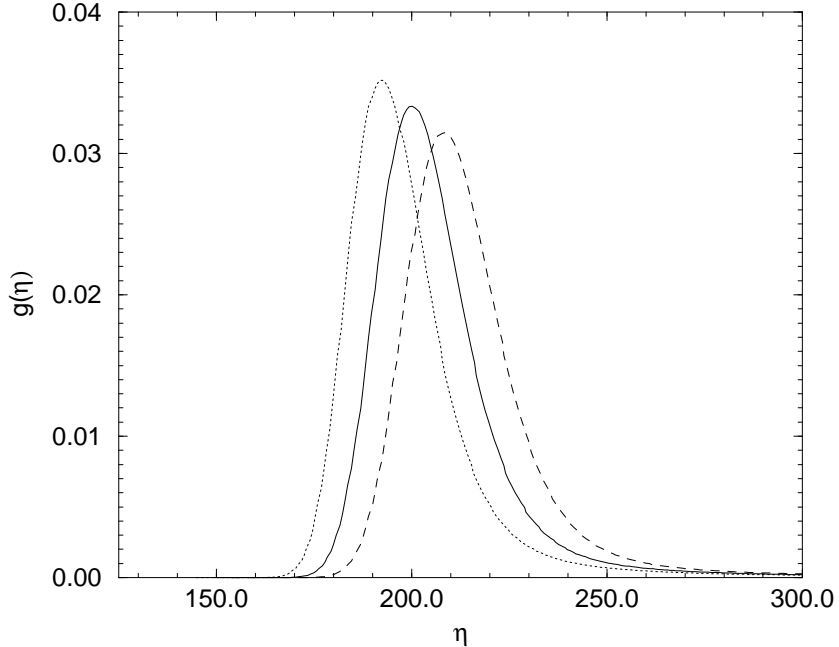


FIG. 3. The visibility function  $g(\eta) = e^{-\tau} d\tau/d\eta$  as a function of conformal time  $\eta$  (in Mpc) for the standard scenario (SCDM,  $\Omega_b = 0.05$ ,  $h = 0.65$ ) (solid curve), an increase of  $\alpha$  by 3% (dotted curve) and a decrease of  $\alpha$  by 3% (dashed curve). The peak of  $g(\eta)$  defines the location of the surface of last scattering and its width defines the thickness of the last scattering surface. As can be seen, increasing  $\alpha$  moves the last scattering surface to higher redshift (smaller conformal time) and decreases its thickness.

Are there any other potential effects on the CMB due to a variation in  $\alpha$ ? One completely negligible effect is the change in the He recombination scenario due to the change in the binding energies of He atomic levels. Another effect is the change in the variation of the matter temperature with time. Specifically, the matter temperature variation consists of adiabatic cooling due to the expansion of the universe and the cooling due to Thomson scattering. The change in  $\sigma_T$  changes the latter. However, the matter temperature accurately tracks the radiation temperature until very late (1% difference at  $z \sim 500$ ) and hence this effect has no consequences for the present purposes.

### III. CHANGES IN THE CMB FLUCTUATION SPECTRUM

We have integrated the changes in the differential optical depth due to a variation in  $\alpha$  into CMBFAST [16]. The results are shown in Fig. 4 for a  $\pm 3\%$  change in  $\alpha$ . Two separate effects may be noted from the results. One, for an increase in  $\alpha$ , the peak positions in the spectrum shift to higher values of  $\ell$ . Two, increasing  $\alpha$  causes the values of  $\mathcal{C}_\ell$  to systematically increase. Conversely, a decrease in  $\alpha$  shifts the peaks to lower values of  $\ell$  and decreases their amplitude.

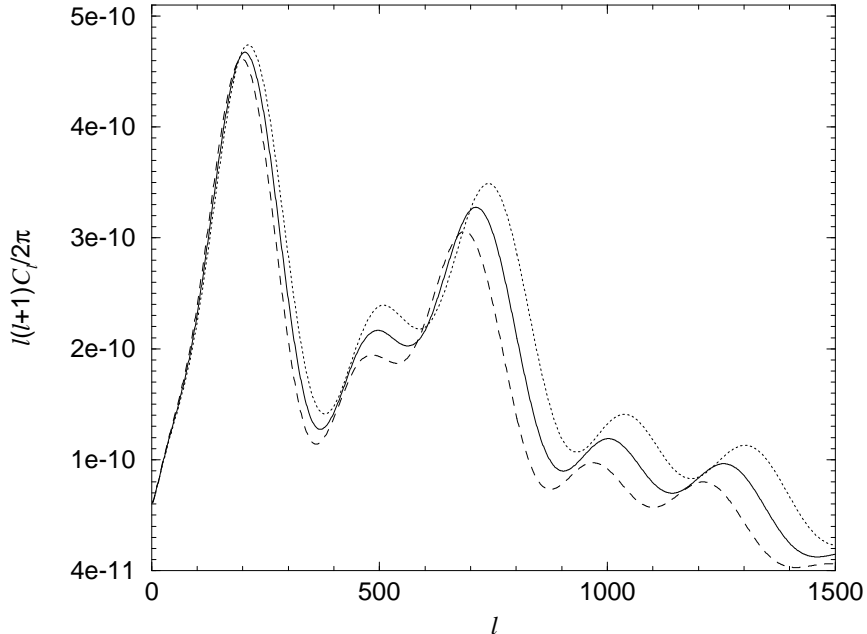


FIG. 4. The spectrum of CMB fluctuations for the standard scenario (SCDM,  $\Omega_b = 0.05$ ,  $h = 0.65$ ) (solid curve), an increase of  $\alpha$  by 3% (dotted curve), and a decrease of  $\alpha$  by 3% (dashed curve)

To understand the first feature, a qualitative understanding of the position of the peaks is necessary. Using  $\ell_p$  to denote the position of a peak,  $r_\theta(z)$  for the angular diameter distance and  $r_s(z)$  for the sound horizon, one can write [17]  $\ell_p \sim r_\theta(z_{ls})/r_s(z_{ls})$ , where  $z_{ls}$  is the redshift of the surface of last scattering. Increasing  $\alpha$  increases the redshift of the last scattering surface, as seen in Fig. 3. A higher redshift at the last scattering surface corresponds to a smaller sound horizon and thus, a higher value of  $l$ . Decreasing  $\alpha$  has the opposite effect: the redshift of last scattering decreases, producing a larger sound horizon at last scattering, and thus a smaller value of  $l$  for the peaks.

The increase in the amplitude of the peaks with increasing  $\alpha$  derives from two separate effects. The amplitude of the first peak is quite sensitive to the magnitude of the integrated Sachs-Wolfe (ISW) effect. If a mode enters the horizon when radiation still makes a significant contribution to the energy density, the decay of the gravitational potential leads to the blueshift of photons [18]. This effect has been dubbed the “early ISW effect” to distinguish it from the decay of the gravitational potential at late times in models which become dominated by curvature or a cosmological constant. An increase in  $\alpha$  pushes recombination to a higher redshift, resulting in a larger early ISW effect and, thus, a larger amplitude of the first peak. The early ISW effect is felt most strongly around the scale of the sound horizon at last scattering. For the SCDM model we have considered, this is around 100 Mpc or  $\ell \sim 100$ . By  $\ell \sim 500$ , the effect of early ISW contributions is negligible.

Beyond the first peak a second effect is dominant: diffusion damping of CMB fluctuations due to the finite thickness of the last scattering surface (see Fig. 3). Because the last-scattering surface is not infinitely thin, the anisotropies seen today are an average over a region of finite thickness defined by the visibility function. This leads to damping of small-scale anisotropies, given by a photon diffusion damping factor averaged over the visibility function [19],

$$D(\lambda) = \int_0^\infty dz g(z) \exp(-\lambda_D^2(z)/\lambda^2) \approx \exp(-\lambda_D^2(z_{ls})/\lambda^2). \quad (10)$$

The characteristic damping length  $\lambda_D$  is set by the width of the visibility function. (The multipole damping scale is given approximately by  $l_D \sim 2H_0^{-1}/\lambda_D$ ). As explained earlier and shown in Fig. 3, the comoving damping length decreases with increasing  $\alpha$ . Thus, an increase in  $\alpha$  decreases the effect of damping, and the power spectrum at large  $l$  increases with increasing  $\alpha$ , as seen in Fig. 4.

#### IV. LIMITS ON VARIATIONS IN THE FINE-STRUCTURE CONSTANT

From the analysis presented in sections II and III, it is clear that a variation in  $\alpha$  has a substantial effect on the CMB fluctuation spectrum. The aim of this section is to obtain a quantitative measure of the limits put on  $\alpha$  by an ideal CMB anisotropy experiment. This can be accomplished through an analysis of the Fisher information matrix. If our estimate of the cosmological parameters ( $\theta_i$ ) is very close to the true values, then the likelihood function ( $\mathcal{L}$ ) can be expanded about its maximum as

$$\mathcal{L} \simeq \mathcal{L}_m \exp(-F_{ij} \delta\theta_i \delta\theta_j), \quad (11)$$

where  $F_{ij}$  is the Fisher information matrix, defined as [20]

$$F_{ij} = \sum_{\ell=2}^{\ell_{\max}} \frac{1}{\Delta\mathcal{C}_\ell^2} \left( \frac{\partial\mathcal{C}_\ell}{\partial\theta_i} \right) \left( \frac{\partial\mathcal{C}_\ell}{\partial\theta_j} \right). \quad (12)$$

In equation (12), the quantity  $\Delta\mathcal{C}_\ell$  is the error in the measurement of  $\mathcal{C}_\ell$ . From the Gaussian form of  $\mathcal{L}$ , the covariance matrix is seen to be  $F^{-1}$ . In particular, one can define the standard deviation for each parameter  $\theta_i$  as  $\sigma_i^2 = (F^{-1})_{ii}$ . The cosmological parameters ( $\theta_i$ ) that need to be determined from the measured fluctuation spectrum are taken to be the Hubble parameter ( $h$ ), the number density of baryons (parametrized as  $\Omega_b h^2$ ), the cosmological constant (parametrized as  $\Omega_\Lambda h^2$ ), the effective number of relativistic neutrino species ( $N_\nu$ ), the primordial helium mass fraction ( $Y_p$ ), and the fine-structure constant ( $\alpha$ ). We make the assumption that the experiments are limited only by the cosmic variance up to a maximum  $\ell$ , denoted by  $\ell_{\max}$ . This assumption is an oversimplification, but it provides a rough upper bound on the possible limits on  $\Delta\alpha/\alpha$  from future CMB experiments.

The fiducial models used for the present work are a standard cold dark matter model (SCDM) and a CDM model with a cosmological constant ( $\Lambda$ CDM). Both models have  $\Omega_b h^2 = 0.02$ ,  $h = 0.65$ ,  $Y_p = 0.246$ , and  $N_\nu = 3.04$ . (Note that various higher-order effects, most notably the slight heating of the  $\nu\bar{\nu}$  pairs by electron-positron annihilation, increase the effective value of  $N_\nu$  to 3.04 from its canonical value of 3 [21]). In the  $\Lambda$ CDM model,  $\Omega_\Lambda$  is taken to be 0.7. We use an adiabatic, scale invariant initial power spectrum and constrain the cosmology to be flat in keeping with the standard inflationary paradigm. For each of these two models, we consider two limiting cases regarding prior constraints on the unknown parameters: first, no prior constraints at all, and second, a “best-case” set of limits on the unknown parameters using priors [22]. In the latter case, we take, as  $1 - \sigma$  limits,  $h = 0.65 \pm 0.05$  from current observations, and  $\Omega_b h^2 = 0.02 \pm 0.002$  and  $Y_p = 0.246 \pm 0.001$  from Big-Bang nucleosynthesis [23]. For this case, we also fixed  $N_\nu$  to be exactly equal to 3.04.

The required derivatives of the  $\mathcal{C}_\ell$ 's were calculated by two-sided finite differencing for each parameter, while the rest were kept fixed. We verified that the changes in the results obtained were less than 10% when the variation of the parameters was halved. The results are shown in Fig. 5 in terms of the ratio  $\sigma_\alpha/\alpha$ , where  $\sigma_\alpha$  is the  $1 - \sigma$  accuracy measure obtained from the Fisher matrix analysis. We see that the estimated upper limits on  $|\Delta\alpha/\alpha|$  vary from about  $10^{-2}$  for  $\ell_{\max} \sim 500 - 1000$  down to  $10^{-3}$  for  $\ell_{\max} > 1500$ .

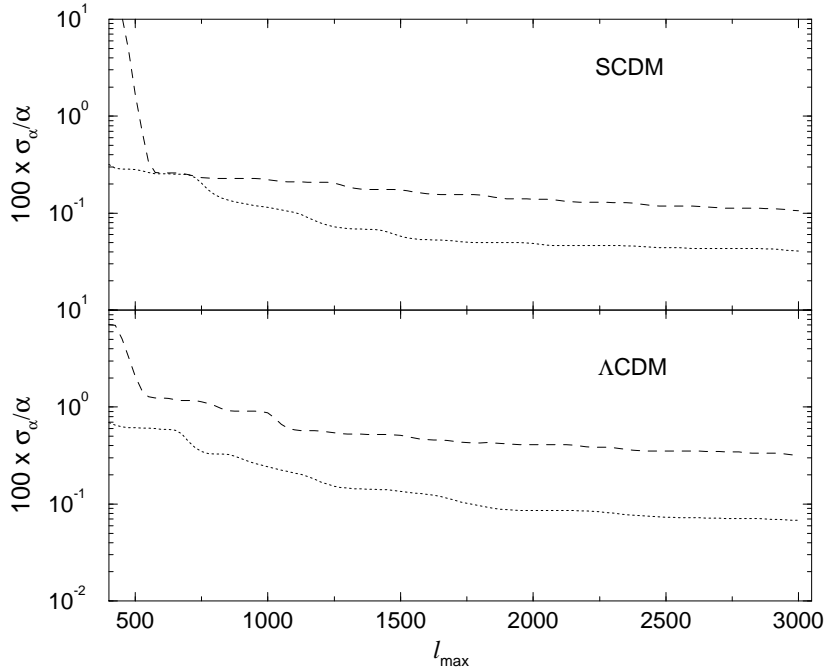


FIG. 5. The estimated accuracy with which  $\alpha$  can be constrained by a cosmic variance limited CMB anisotropy experiment, as a function of the maximum angular resolution given by  $\ell_{max}$ . The dotted curve is the result of including priors as explained in the text, while the dashed curve is for the case without priors.

These results suggest that future CMB experiments (MAP and PLANCK) might be able to constrain any variation in the fine-structure constant to less than  $10^{-2} - 10^{-3}$ . This is a weaker constraint than can be obtained from current quasar absorption studies, but the CMB limit would apply at a much higher redshift ( $z \sim 1000$ ). It represents a much more direct and reliable constraint than the only other limit at  $z \gg 1$ , available from Big Bang nucleosynthesis [7].

We are grateful to A. Heckler and S. Carroll for helpful discussions, and we thank A. Heckler for the use of his CMB Fisher matrix code. We thank U. Seljak and M. Zaldarriaga for the use of CMBFAST [16]. This work was supported in part by NASA (NAG 5-2788) at Fermilab and by the DOE at Fermilab, Chicago and Ohio State (DE-FG02-91ER40690).

- 
- [1] P.A.M. Dirac, Nature (London) **139**, 323 (1937).
  - [2] J.D. Prestage, R.L. Tjoelker, & L. Maleki, Phys. Rev. Lett. **74**, 3511 (1995).
  - [3] M.J. Drinkwater, J.K. Webb, J.D. Barrow, & V.V. Flambaum, MNRAS **295**, 457 (1998).
  - [4] L.L. Cowie & A. Songaila, Astrophys. J. **453**, 596 (1995).
  - [5] J.K. Webb, V.V. Flambaum, C.W. Churchill, M.J. Drinkwater, & J.D. Barrow, astro-ph/9803165.
  - [6] T. Damour & F. Dyson, Nucl. Phys. B **480**, 37 (1996).
  - [7] E.W. Kolb, M.J. Perry, & T.P. Walker, Phys. Rev. D **33**, 869 (1986).
  - [8] W. Marciano, Phys. Rev. Lett. **52**, 489 (1984).
  - [9] S.M. Carroll, astro-ph/9806099, and private communication.
  - [10] P. J. E. Peebles, Astrophys. J. **153**, 1 (1968)
  - [11] B. J. T. Jones & R. F. G. Wyse, A&A **149**, 144 (1985)
  - [12] L. Spitzer & J. L. Greenstein, Astrophys. J. **114**, 407 (1951)
  - [13] W. J. Boardman, Astrophys. J. Supp. **9**, 185 (1964)
  - [14] G. Breit & E. Teller, Astrophys. J. **91**, 215 (1940)



- [15] P. Boschán & P. Biltzinger, astro-ph/9611032
- [16] U. Seljak and M. Zaldarriaga, *Astrophys. J.* **469**, 437 (1996).
- [17] W. Hu, 'UC Berkeley Ph.D. Thesis' (May 1995), astro-ph/9508126
- [18] W. Hu, N. Sugiyama & J. Silk, *Nature* **386**, 37 (1997).
- [19] W. Hu & M. White, *Astrophys. J.* **479**, 568 (1997).
- [20] M. Tegmark, A. Taylor & A. F. Heavens, *Astrophys. J.* **480**, 22 (1997)
- [21] R.E. Lopez, S. Dodelson, A. Heckler, & M.S. Turner, astro-ph/9803095.
- [22] J. R. Bond, G. P. Efstathiou & M. Tegmark, *MNRAS* **291**, L31 (1997)
- [23] D.N. Schramm & M.S. Turner, *Rev. Mod. Phys.* **70**, 303 (1998); S. Burles & D. Tytler, *Astrophys. J.* **499**, 699 (1998); *Astrophys. J.* , in press (1998)